Optimisation of inductive energy transmission systems with an extraordinarily large air gap

Dr.-Ing. Rudolf Mecke
Institut f. Automation u. Kommunikation Magdeburg
Steinfeldstraße 3, D-39179 Barleben, Germany
Tel.: +49 39203 81054, Fax: +49 39203 81100, e-mail: rme@ifak.fhg.de

Keywords

Flux model, Magnetic devices, Power transmission, Systems engineering

Abstract

Inductive energy transmission through a large air gap is becoming more and more attractive especially for automatic battery charging stations and for energy supply of inductively powered electric vehicles and other movable consumers. The paper investigates the influence of geometrical and electrical parameters on energy transmission through air gaps of several hundred millimetres. The investigations are carried out by means of magnetic flux simulation and measurements. The transferable electric power and the efficiency of magnetic assemblies with large air gaps can be considerably improved by using higher transmission frequencies in the range of several hundred kilohertz.

1 Introduction

The contactless inductive energy transmission technology has been developed within the last few years. Typical applications are robots, machine tools, linear movable systems and non-contact battery chargers for electric vehicles. By means of the contactless transmission technology, trailing cables can be replaced and therefore cable breaks can be avoided. Other advantages are: no wear and tear on the electrical contacts, no contact resistance, no sparking (can be used in explosion-endangered environment) and no non-protected voltage-carrying contacts. A common feature of all applications for which the contactless energy transmission has been used for up to now, is the relatively small air gap (in the range of several millimetres) between the primary and secondary system. Therefore, such magnetic assemblies can be accurately described by means of commonly known magnetic equations. However, for some applications which are becoming more interesting for the future (for example inductively powered electric vehicles, automatic battery charging stations), an extraordinarily large air gap of several hundred millimetres is desired. The extension of the contactless energy transmission to longer distances opens new application fields for this electricity supply technology.

2 Model of the magnetic system

Extensive investigations in the frequency range of up to 200 kHz have shown that the steady-state as well as the dynamic behaviour of any magnetic assembly with a large air gap can be described by the equivalent electric circuit in Fig. 1. The electric circuit in Fig. 1 contains the main inductance L_h, the leakage inductances $L_{1\sigma}$, $L_{2\sigma}$, the ohmic resistances of the windings (R_1, R_2) and the secondary load resistance R_L. The parameters of the secondary coil are transformed to the primary side according to the transformer turns ratio.

The inductances L_h, $L_{1\sigma}$ and $L_{2\sigma}$ can be obtained by means of a magnetic flux simulation. Starting from the magnetic flux distribution (Fig. 2), the inductances can be calculated as described in the following equations:

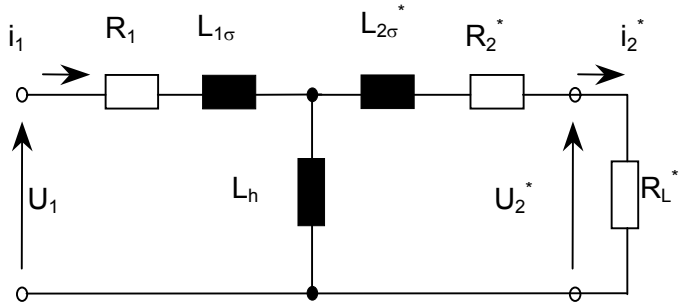

Fig. 1: Equivalent electric circuit of a contactless inductive transmission system

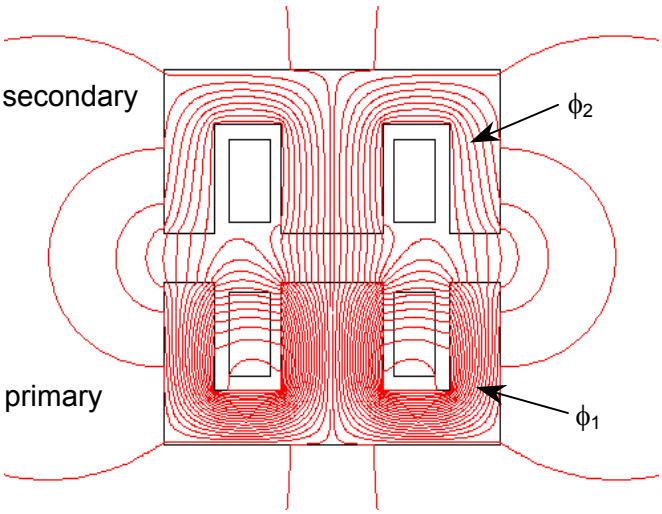

Fig. 2: Magnetic flux lines of a contactless energy transmission assembly

At first only the primary coil is fed by the current i_{1NL}. As a result of the magnetic flux simulation, the fluxes ϕ_{1NL} and ϕ_{2NL} can be obtained and by means of the equations (1) and (2), the main inductance and the primary leakage inductance can be calculated.

$$L_h = N_1^2 \cdot \frac{\hat{\phi}_{2NL}}{\hat{i}_{1NL}} \tag{1}$$

$$L_{1\sigma} = N_1^2 \cdot \frac{\hat{\phi}_{1NL} - \hat{\phi}_{2NL}}{\hat{i}_{1NL}} \tag{2}$$

In a second simulation the primary and secondary coils are fed by the currents i_{1L} and i_{2L} which have opposite directions. The secondary leakage inductance can be obtained by means of the fluxes ϕ_{1L} and ϕ_{2L} as shown below:

$$L_{2\sigma} = N_2^2 \cdot \frac{\hat{\phi}_{1L} - \hat{\phi}_{2L} - L_{1\sigma}\hat{i}_{1L}}{\hat{i}_{2L}} \tag{3}$$

The following table compares the calculated and measured inductances of a magnetic assembly with an air gap of 100 mm. The correspondence between the calculation and measurement is good up to a transmission frequency of 200 kHz. In general, magnetic assemblies with an air gap are characterised by a very small main inductance and large leakage inductances, compared to assemblies with no an air gap. This means, for the generation of a magnetic flux used for energy transmission, a high primary

current is necessary. This primary current causes considerable copper losses and reduces the overall efficiency.

	L_h [µH]	$L_{1\sigma}$ [µH]	$L_{2\sigma}$ [µH]
simulation	194	508	508
meas., 20 kHz	190	520	495
meas., 50 kHz	197	515	491
meas., 100 kHz	204	516	491
meas., 200 kHz	228	522	491

3 Inductances

The investigations have shown that the main inductance and the leakage inductances of contactless systems mainly depend on the dimensions of the primary and secondary system, the existence of ferrite cores on the primary or secondary side and the air gap length. Especially for energy transmission over a large air gap (several hundred millimetres), a careful geometrical optimisation is necessary. An optimised magnetic assembly is shown in Fig. 3. The primary and secondary are flat coils with a height of 2 mm and consist of 58 turns litz wire. Each coil is glued onto a ferrite plate.

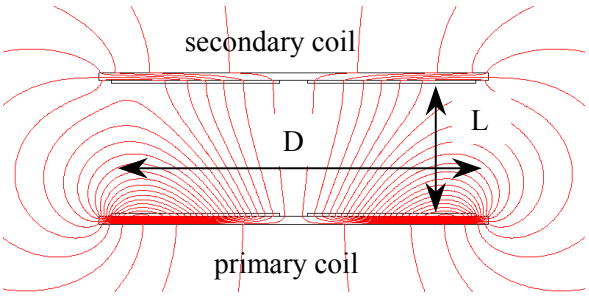

Fig. 3: Optimised magnetic assembly with a large air gap

The main inductance as well as the coil inductance for this magnetic assembly is shown in Fig. 4 and Fig. 5 for different coil diameters as a function of air gap length. The coil inductance of the primary or secondary is the sum of the main inductance and the correspondend leakage inductance. The inductances which are drawn in the graphs (L_{h0}, L_{10}, L_{20}) are related to one winding.

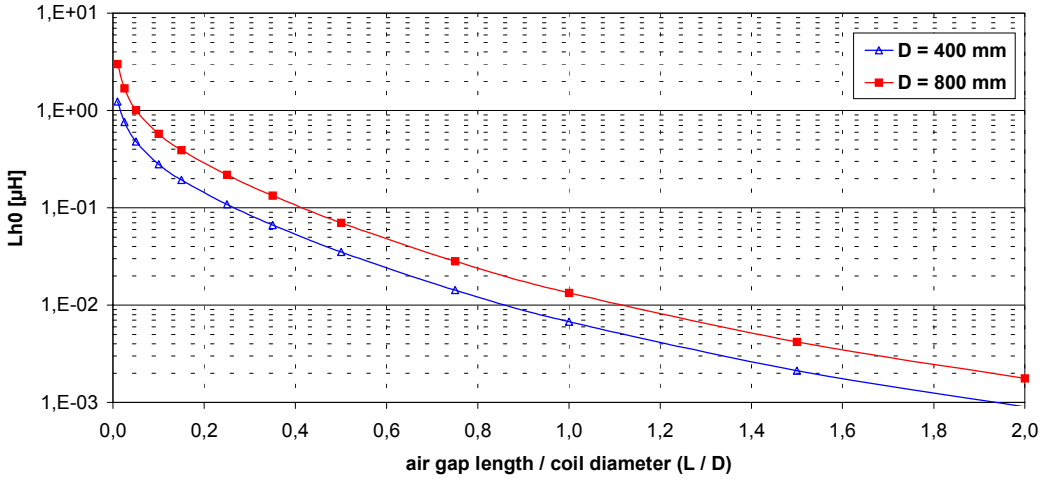

Fig. 4: Main inductance between flat coils as a function of air gap length

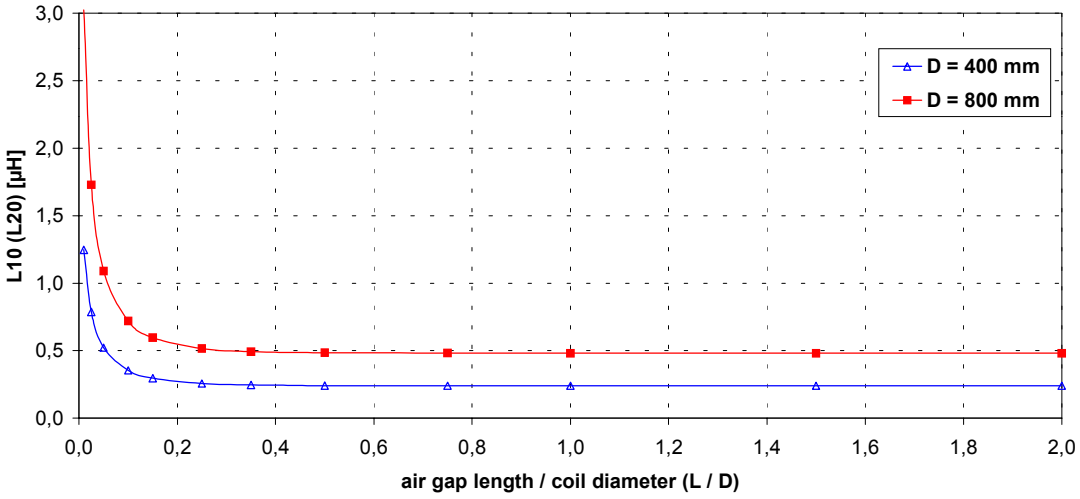

Fig. 5: Primary (secondary) inductance of flat coils as a function of air gap length

As one can observe, the main inductance rapidly decreases with the air gap length. The main inductance as well as the primary and secondary coil inductances are proportional to the coil diameter. For small air gaps, the coil inductances depend on the air gap length. However, for relatively large air gaps (L/D > 0,3), the inductances are nearly constant due to the low magnetic coupling between the primary and secondary coil.

4 Leakage inductance compensation

A fundamental problem of contactless energy transmission systems is the large secondary leakage inductance. It causes a load-dependent secondary voltage drop and therefore a considerable limitation of the transferable electric power. Consequently, the transfer of appreciable electric power in the range above several hundred watts requires the compensation of the secondary leakage inductance. The compensation can be realised either by a parallel resonance capacitor or by a series resonance capacitor at the secondary coil. The best mathematical description is reached for parallel resonance. The transfer function between the primary input current and the secondary output voltage is shown in equation (4).

$$\frac{\widetilde{U}_2^*}{\widetilde{i}_1} = \frac{K \cdot p}{1 + 2d\tau_0 p + \tau_0^2 p^2} \tag{4}$$

The resonance capacitor is nearly independent from the secondary load resistance and can be determined by means of equation (5). A characteristic feature is the damping at the resonance point (equation (6)). Especially at large air gap systems is the damping very low. Therefore, a small variation in transmission frequency would cause a considerable output voltage drop.

$$C_2 = \frac{1 + \dfrac{R_2}{R_L}}{N_2^2 \left(L_{h0} + L_{2\sigma 0}\right) \cdot \omega_{res}^2} \tag{5}$$

$$d = \frac{N_2^2 \left(L_{h0} + L_{2\sigma 0}\right) + R_2 R_L C_2}{2N_2 \sqrt{C_2 R_L \left(R_L + R_2\right)\left(L_{h0} + L_{2\sigma 0}\right)}} \tag{6}$$

For operation at resonance frequency, the output power is contained in equation (8) and the efficiency in equation (9) as function of the secondary load resistance. The ohmic resistances (R_{10}, R_{20}) are calculated for one winding according to equation (7).

$$R_1 = N_1^2 \cdot R_{10} \quad ; \quad R_2 = N_2^2 \cdot R_{20} \tag{7}$$

$$P_2 = \left(N_1 \tilde{i}_1 \frac{L_{h0}}{N_2 \left(L_{h0} + L_{2\sigma 0}\right) + \dfrac{R_{20} R_L}{N_2 \left(L_{h0} + L_{2\sigma 0}\right) \omega_{res}^2}} \right)^2 R_L \tag{8}$$

$$\eta = \frac{R_L}{R_L + \dfrac{R_{10}\left[N_2^2 \left(L_{h0} + L_{2\sigma 0}\right)^2 \omega_{res}^2 + R_{20} R_L\right]^2}{N_2^2 L_{h0}^2 \left(L_{h0} + L_{2\sigma 0}\right)^2 \omega_{res}^4} + N_2^2 R_{20} \left[1 + \left(\frac{R_L}{N_2^2 \left(L_{h0} + L_{2\sigma 0}\right) \omega_{res}} \right)^2 \right]} \tag{9}$$

5 Energy transmission behaviour

5.1.1 General considerations

Fig. 6 shows the output power (equation (8)) and the efficiency (equation (9)) of a contactless energy transmission system as a function of the secondary load resistance. A transmission frequency of 50 kHz is used. The primary and secondary of the magnetic system consist of flat coils (Fig. 3) with a coil diameter of 400 mm each and an air gap length of 400 mm between the two coils. The output power is related to the square of the primary magnetomotive force $(N_1 * i_1)^2$. For further calculations the following assumptions were made: constant ohmic resistances of the windings (no skin and proximity effects), no iron losses. The output power as well as the efficiency in Fig. 6 have a maximum at different load resistances. These two operation points are analysed in detail in the following paragraph.

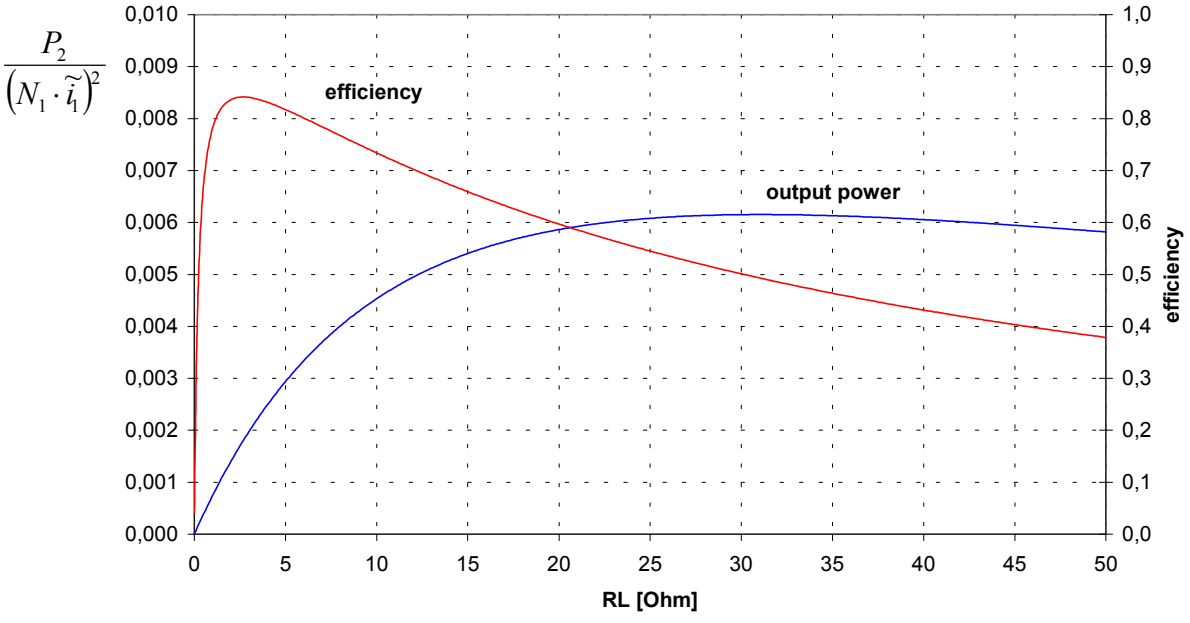

Fig. 6: Output power and efficiency as a function of secondary load resistance

5.1.2 Maximum output power

The operation point at which the maximum output power is reached is described by the equations (10) to (12).

$$R_L = \frac{N_2^2 \left(L_{h0} + L_{2\sigma 0}\right)^2 \omega_{res}^2}{R_{20}} \tag{10}$$

$$P_{2\max} = \left(N_1 \, \tilde{i}_1\right)^2 \cdot \frac{L_{h0}^2}{4 \, R_{20}} \cdot \omega_{res}^2 \tag{11}$$

$$\eta = \frac{1}{2 + \frac{4 \, R_{10} R_{20}}{L_{h0}^2 \, \omega_{res}^2} + \left(\frac{R_{20}}{\left(L_{h0} + L_{2\sigma 0}\right) \omega_{res}} \right)^2} \tag{12}$$

The maximum output power depends on the square of the primary magnetomotive force, the main inductance and the transmission frequency. The output power is limited by the ohmic resistance of the secondary coil. For given geometric parameters of the magnetic assembly, the output power can only be increased by using higher transmission frequencies. At higher frequencies, the increase of the secondary ohmic resistance due to the skin effect has to be regarded. As equation (12) shows, the efficiency at this operation point is below 50 %. Therefore, the maximum output power operation point should not be favourised for energy transmission.

5.1.3 Maximum efficiency

The maximum efficiency can be realised by using the secondary load resistance in equation (13). This value is used as input for the calculation of output power and efficiency by means of the equations (8) and (9).

$$R_L = N_2^2 \left(L_{h0} + L_{2\sigma 0}\right) \omega_{res}^2 \sqrt{\frac{R_{10} \left(L_{h0} + L_{2\sigma 0}\right)^2 + R_{20} L_{h0}^2}{R_{10} R_{20}^2 + R_{20} L_{h0}^2 \omega_{res}^2}} \tag{13}$$

The output power and the efficiency at this operation point cannot be described easily by equations. Therefore these values have to be shown in diagrams.

Fig. 7 shows the output power of the magnetic system (Fig. 3) with a coil diameter of 800 mm as a function of air gap length. The primary magnetomotive force (N_1*i_1) is set to 1500 A. The investigations are carried out for different transmission frequencies. The reachable output power strongly decreases with the air gap length nearly in the same way as the main inductance (Fig. 4).

The output power for different air gap lengths as a function of transmission frequency is shown in Fig. 8. The output power can be increased by using higher transmission frequencies. For example, an electric power of 20 kW can be transferred over an air gap of 800 mm by using a transmission frequency of 100 kHz. The efficiency of the magnetic assembly is mainly influenced by the transmission frequency. Fig. 9 shows the efficiency of a magnetic assembly for different air gap lengths as a function of transmission frequency. The comparison shows the reduction of efficiency with an increasing air gap due to the low magnetic coupling. However, the efficiency of a magnetic assembly with a large air gap (for example 1600 mm) can be improved by using higher transmission frequencies in the range of several hundred kilohertz. For smaller air gap lengths, below 800 mm in this case, the efficiency is greater than 90 % already at low transmission frequencies.

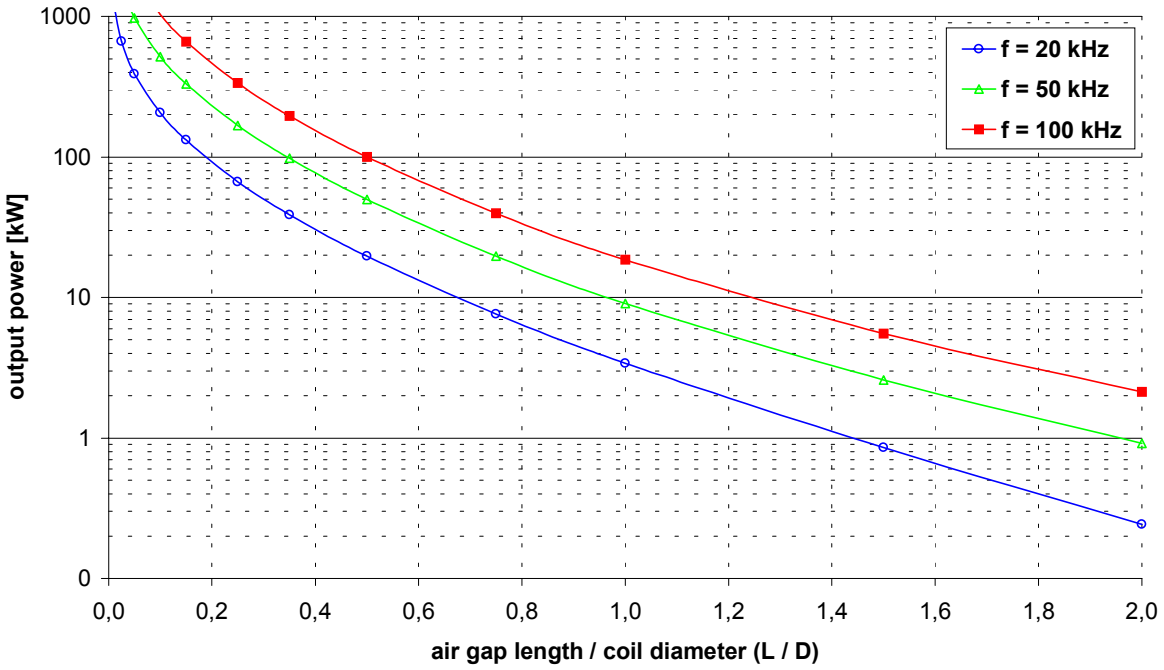

Fig. 7: Output power for different transmission frequencies as a function of air gap length

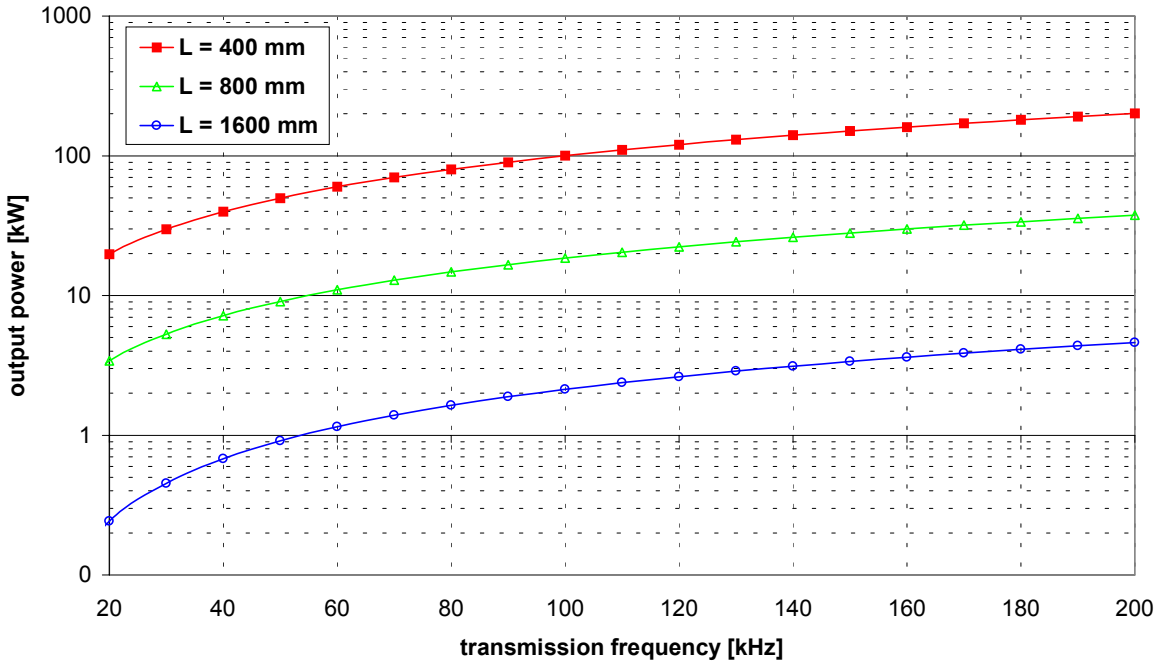

Fig. 8: Output power for different air gap lengths as a function of transmission frequency

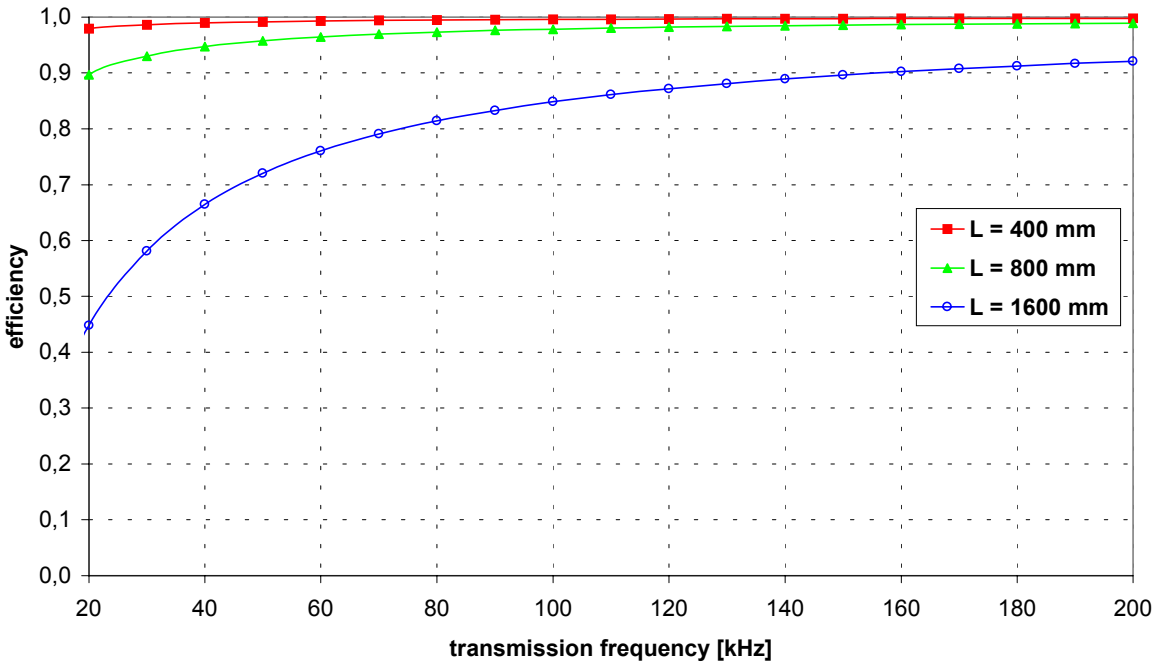

Fig. 9: Efficiency for different air gap lengths as a function of transmission frequency

6 Conclusion

The steady-state and dynamic behaviour of contactless energy transmission systems can be described by means of the equivalent electric circuit of a transformer in the frequency range of up to 200 kHz. Such systems are characterised by a small main inductance and large leakage inductances. The inductances can be obtained by a magnetic flux simulation. The energy transmission behaviour mainly depends on the dimensions of the primary and secondary system, the existence of ferrite cores on the primary or secondary side and the air gap length. Especially for energy transmission over a large air gap, a careful geometrical optimisation of the magnetic system is necessary. The transmission frequency mainly influences the transferable electric power and the efficiency. Good efficiency of large air gap systems requires high transmission frequencies of at least 100 kHz. The investigations are carried out for air gap lengths of up to 1600 mm and a power range of several kilowatts. An efficiency greater than 90 % can be realised for the magnetic system.

7 Acknowledgments (optional)

The proposed work is supported by the Ministry of Education and the Arts of Saxony-Anhalt.

8 References

1. Eßer, A.; Nagel, A.: Contactless high speed signal transmission integrated in a compact rotatable power transformer. European Conference on Power Electronics and Applications, Brighton 1993, Vol. 4, pp 409-414
2. Green, A. W.; Boys, J. T.: 10 kHz inductively coupled power transmission – concept and control. International Conference on Power Electronics and Variable Speed Drives, London 1994, pp 694-699
3. Knaup, P.; Hasse, K.: Zero voltage switching converter for magnetic transfer of energy to movable systems. European Conference on Power Electronics and Applications, Trondheim 1997, Vol. 2, pp 168-173
4. Hayes, J. G.; Hall, J. T.; Bellino, G.; Conroy, K.: Off-board incuctive charging for the Genaral Motors EV1 electric vehicle. International Electric Vehicle Symposium, Brüssel 1998, Proceedings on CD-ROM
5. Klontz, K. W.; Divan, D. M.; Novotny, D. W.; Lorenz, R. D.: Contactless power delivery system for mining applications. IEEE Transactions on Industry Applications, Vol. 31, No. 1, January/February 1995, pp 27-35

6. Jufer, M.; Macabrey, N.; Perrottet, M.: Modeling and test of contactless inductive energy transmission. International Conference Electrimacs, Saint-Nazaire 1996, Vol. 3, pp 1199-1204

7. Nishimura, T. H.; Eguchi, T.; Inoue, T.; Hirachi, K.; Maejima, Y.; Saito, M.: An analysis of a large air gap transformer by using a transcutaneous energy transmission. European Conference on Power Electronics and Applications, Sevilla 1995, Vol. 2, pp 317-322

8. Knaup, P.: Berührungslose Energie-übertragung auf linear bewegte Systeme. PhD Thesis TU Darmstadt, 1999

9. Barnard, J. M.; Ferreira, J. A.; van Wyk, J. D.: Optimising sliding transformers for contactless power transmission systems. Power Electronics Specialists Conference, 1995, pp 245-251